

# The Hubble Tension as an Inference-Bias Signal: Dark Sirens with Modified Gravitational-Wave Propagation

Aiden B. Smith<sup>1\*</sup>

<sup>1</sup>Independent Researcher

## ABSTRACT

The Hubble tension is commonly interpreted as a mismatch in expansion history between early- and late-universe probes. If gravitational-wave (GW) luminosity distances deviate from electromagnetic distances through modified propagation, then applying a GR standard ruler introduces an inference bias in  $H_0$ . Motivated by the recently reported GWTC-3 dark-siren propagation posterior, treated here as a phenomenological template, we propagate this effect through a Planck-facing modified-gravity recalibration and obtain  $H_0^{\text{Planck, MG}} = 68.0$ ,  $\Omega_m^{\text{Planck, MG}} = 0.306$ , and  $A_{\text{lens}} = 1.04$ .

GR standard-ruler inversion of MG-consistent draws yields a tension-scale shift: mean  $\Delta H_0 = +1.9 \text{ km s}^{-1} \text{ Mpc}^{-1}$  for fixed  $\Omega_m$  and  $+4.6 \text{ km s}^{-1} \text{ Mpc}^{-1}$  for a lensing-proxy  $\Omega_m$ . Direct late-time friction closure is smaller ( $\mathcal{R}_{\text{anchor}}^{\text{GR}} = 0.155$ ). Baseline CAMB projection predicts suppressed CMB lensing, while an MG-aware response refit restores near-reference quality (median  $\chi^2 = 8.1$  versus 9.0 for the Planck reference). An amplitude dial,  $R_\alpha(z) = 1 + \alpha [R(z) - 1]$ , indicates cross-channel consistency near  $\alpha \simeq 0.6$ , whereas material relief at 0.30 would require  $\alpha \simeq 2$  under linear coupling.

This Letter is an implications analysis: if a propagation deviation of this form is confirmed, corrected dark-siren inference aligns with a Planck-like anchor and GR propagation is not a neutral assumption in standard-siren cosmology.

**Key words:** cosmology: theory – gravitational waves – cosmological parameters – distance scale

## 1 INTRODUCTION

The Hubble-constant tension between late-time distance-ladder measurements and early-universe CMB inference remains a central unresolved issue in precision cosmology (Riess et al. 2022; Freedman et al. 2019; Aghanim et al. 2020a). The standard interpretation is a genuine discrepancy in expansion history. Here we test a different possibility: part of the tension is an *inference bias* generated by applying GR compression to data that follow modified-gravity (MG) propagation.

Motivated by the GWTC-3 dark-siren propagation anomaly reported in our O3 analysis release (Smith 2026), this Letter quantifies the cosmological parameter bias that would be induced if the inferred propagation history is physical. The propagation posterior is used as a phenomenological template; establishing its origin and robustness against catalogue/selection and waveform systematics is treated as a separate problem. Modified GW propagation with an evolving effective Planck mass has long been studied as a viable MG signature (Belgacem et al. 2018; Nishizawa 2018).

In scalar-tensor/EFT constructions, the same running effective Planck mass  $M_*(z)$  that modifies GW amplitudes can also affect background and lensing channels (Bellini & Sawicki 2014; Pogosian & Silvestri 2016). Three questions

are addressed: how much late-time relief remains after recalibrating the sound-horizon anchor; whether Planck 2018 lensing necessarily rejects the implied suppression or can be accommodated by MG response freedom; and how large a GR standard-ruler inversion bias in  $H_0$  is induced when MG truth is assumed.

## 2 METHODOLOGY

Posterior draws from the O3 propagation template are propagated through four linked computations. First, a 60-restart Planck+MG recalibration establishes an updated sound-horizon anchor. Secondly, constrained transfer sweeps are rebased to that anchor and recompressed into a final relief posterior. Thirdly, draw-level CAMB projection to the Planck 2018 lensing bandpowers is performed, followed by an MG-aware two-parameter lensing response refit. Finally, the GR standard-ruler inversion of  $\theta_* = r_d/D_M(z_*)$  is applied under fixed- $\Omega_m$  and lensing-proxy- $\Omega_m$  assumptions to isolate the model-assumption bias. These are targeted cosmological forecasts and refits, not a full MG TT/TE/EE perturbation-likelihood analysis.

\* E-mail: aidenblakesmithtravel@gmail.com

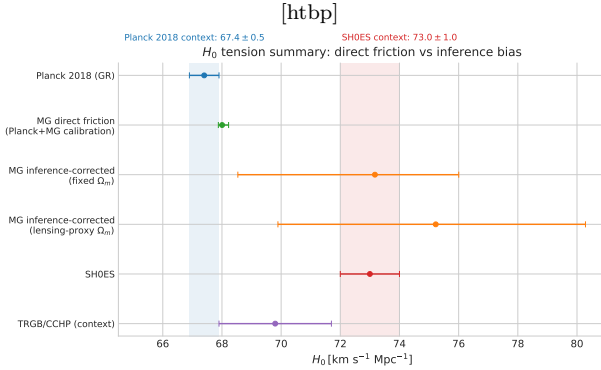


**Figure 1.**  $H_0$  tension summary comparing Planck 2018 (GR), direct-friction recalibration, two GR-inversion bias channels, and local-distance-ladder context (SHOES and TRGB/CCHP (Riess et al. 2022; Freedman et al. 2019)). The dominant displacement comes from GR standard-ruler inversion bias when MG truth is assumed; the broad lensing-proxy interval is the expected  $H_0$ - $\Omega_m$  degeneracy once the artificial  $\Lambda$ CDM standard-ruler rigidity is relaxed.

### 3 RESULTS

#### 3.1 Recalibrated sound-horizon anchor

The 60-restart Planck+MG run completed all restarts with 5 converged minima and 55 max-evaluation exits. Using converged minima only, we obtain:

$$\begin{aligned} H_0^{\text{Planck, MG}} &= 68.01 \text{ (p50)}, \\ \Omega_m^{\text{Planck, MG}} &= 0.3064 \text{ (p50)}, \\ A_{\text{lens}} &= 1.043 \text{ (p50)}. \end{aligned} \quad (1)$$

With local reference  $H_0^{\text{local}} = 73.0$ , the baseline gap used in rebased relief calculations is

$$\Delta H_0^{\text{base}} = |H_0^{\text{local}} - H_0^{\text{Planck, MG}}| = 4.99. \quad (2)$$

#### 3.2 Inference bias from GR standard-ruler inversion

To isolate model-assumption bias, we treat MG posterior draws as truth and invert  $\theta_* = r_d/D_M(z_*)$  with a GR compression model. For fixed  $\Omega_m = \Omega_m^{\text{Planck, MG}}$ , we obtain  $H_0$ ,inferred mean 72.39 (p50 73.17), corresponding to mean  $\Delta H_0 = +1.88 \text{ km s}^{-1} \text{ Mpc}^{-1}$  relative to draw-level truth. For a lensing-proxy  $\Omega_m$  compression,  $H_0$ ,inferred mean is 75.07 (p50 75.23), giving mean  $\Delta H_0 = +4.55 \text{ km s}^{-1} \text{ Mpc}^{-1}$ . The wider lensing-proxy interval reflects the expected  $H_0$ - $\Omega_m$  degeneracy once the artificial rigidity of the  $\Lambda$ CDM standard ruler is removed; in this channel, the analysis releases model-imposed precision rather than exhibiting numerical instability. In physical terms, GR inversion acts as an *invisible wedge*: it pushes inferred anchors upward when the underlying propagation is MG-like.

Relative to the recalibrated Planck+MG anchor  $H_0^{\text{Planck, MG}} = 68.01$ , the posterior medians shift by:

$$\begin{aligned} \Delta H_0^{\text{truth}} &\approx +2.39, \\ \Delta H_0^{\text{fixed inversion}} &\approx +5.16, \\ \Delta H_0^{\text{lensing inversion}} &\approx +7.22 \text{ km s}^{-1} \text{ Mpc}^{-1}. \end{aligned} \quad (3)$$

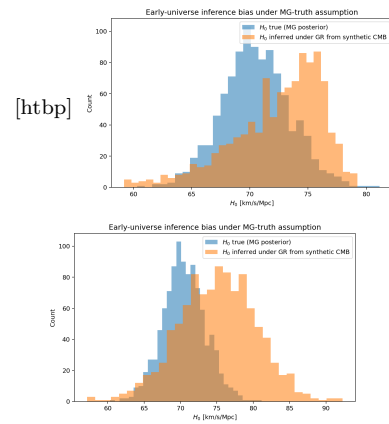


**Figure 2.** Draw-level  $H_0$  truth versus GR-inferred  $H_0$  under compressed standard-ruler inversion with fixed- $\Omega_m$  (left) and lensing-proxy- $\Omega_m$  (right). Both assumptions bias inferred  $H_0$  upward, with larger displacement in the lensing-proxy case.

#### 3.3 Direct friction relief and late-time rebasing

After rebasing constrained transfer sweeps to the updated sound-horizon calibration anchor and applying Monte Carlo calibration:

$$\mathcal{R}_{\text{anchor}}^{\text{GR}} = 0.155. \quad (4)$$

The corresponding posterior summary is p16/p50/p84 = 0.108/0.147/0.189.

Two independent robustness and joint-fit diagnostics are as follows. A 10-case robustness grid gives posterior-shift relief mean 0.530 (p50 0.513, p84 0.545), with zero failed cases. A joint SN+BAO+CC transfer fit gives relief posterior mean 0.833 (p50 0.839), but

$$\log \text{BF}_{\text{transfer/no-transfer}} = -0.53, \quad (5)$$

so explicit transfer terms are not favoured in this setup. The high- $z$  transfer-bias sensitivity map used for calibration has been moved to supplemental material (Fig. S1).

#### 3.4 CMB lensing: baseline suppression and MG-aware response freedom

Baseline draw-level CAMB projection against Planck 2018 lensing bandpowers (`consext8`, 64 draws) gives:

$$\left. \frac{C_L^{\phi\phi}(\text{MG})}{C_L^{\phi\phi}(\text{Planck ref})} \right|_{L \approx 106} = 0.847^{+0.091}_{-0.127}, \quad (6)$$

$$\left. \frac{C_L^{\phi\phi}(\text{MG})}{C_L^{\phi\phi}(\text{Planck ref})} \right|_{L \approx 286} = 0.905^{+0.068}_{-0.080}, \quad (7)$$

with median suppressions of  $-15.29\%$  and  $-9.49\%$ . The baseline fit quality is poor relative to the Planck-reference model:

$$\chi^2_{\text{MG, baseline}} (\text{median}) = 51.77, \quad \chi^2_{\text{Planck ref}} = 9.04, \quad (8)$$

and only 3.1% of draws outperform the reference. A 32-draw cross-check from an independent posterior sample is more discrepant ( $-18.66\%$  at  $L \approx 106$ ,  $-11.29\%$  at  $L \approx 286$ ;  $p_{\text{better}} = 0$ ).

To test whether this baseline mismatch is rigid, we perform

an MG-aware lensing refit (32 draws) with a phenomenological effective- $M_\star^2$  amplitude plus  $\ell$ -tilt response. This freedom is motivated by scalar-tensor/EFT treatments where matter-growth and light-deflection responses need not track identically and can acquire scale dependence (Bellini & Sawicki 2014; Pogosian & Silvestri 2016). The refit removes the baseline mismatch:

$$\chi_{\text{MG refit}}^2 (\text{median}) = 8.06, \quad (9)$$

better than the Planck-reference  $\chi^2 = 9.04$  in 100% of refit draws. This refit is phenomenological and demonstrates model-class freedom, not a unique derivation of one covariant MG Lagrangian. The fitted median response corresponds to

$$\frac{M_\star^2(z=0)}{M_\star^2(z \gg 1)} \simeq 0.901 \quad (10)$$

(about a 9.9% drop), with small residual suppression at  $L \approx 286$ .

### 3.5 Constraints on propagation amplitude

To quantify how strongly the reconstructed propagation signal must scale to satisfy cross-probe consistency criteria, we ran a lightweight amplitude dial around the current posterior signal:

$$R_\alpha(z) = 1 + \alpha [R(z) - 1]. \quad (11)$$

Using existing growth, lensing, and distance-ratio consistency summaries as a fast emulator (not a full re-inference at each  $\alpha$ ), we find: the distance-ratio criterion passes at  $\alpha \approx 0.18$ ; the growth criterion passes at  $\alpha \approx 0.58$ ; the lensing-growth consistency criterion passes at  $\alpha \approx 0.60$ ; and the combined support criterion (M2) turns on at  $\alpha \approx 0.60$ . For the material-relief requirement ( $\mathcal{R}_{\text{anchor}}^{\text{GR}} \geq 0.30$ ), two cases are informative: (i) if relief is held fixed at the current calibrated level, no solution appears for  $\alpha \in [0, 3]$ ; (ii) under linear relief coupling,  $\mathcal{R}_{\text{anchor}}(\alpha) \propto \alpha$ , the threshold is crossed at  $\alpha \approx 1.95$ . This gives a simple scale estimate: core cross-channel support is compatible with the present signal level, while material closure needs roughly a factor-of-two stronger effective propagation amplitude under linear coupling.

### 3.6 Cross-probe and stability checks

We also ran lightweight forward checks to test whether the current signal can be embedded in a broader predictive picture without adding new heavy global fits. These checks satisfy the three core consistency criteria used here: bridge solutions exist, the dark-siren preference survives high-leverage-event removal, and the SN-only transfer channel remains same-sign. Finally, we performed a waveform-level likelihood-consistency check on the two highest-leverage events (GW200308\_173609 and GW200220\_061928) using public GWOSC O3 strain. We evaluated the extrinsic-marginalised likelihood with the RIFT engine across multiple random seeds and two independent waveform families (IMRPhenomPv3HM and IMRPhenomXPHM). All 10 runs completed without numerical failures. This does not constitute a full alternative PE or a glitch analysis, but it reduces the plausibility that the population-level preference is driven by a gross waveform-evaluation pathology in the dominant events.

**Pantheon inference-bias audit.** In an SN-only transfer model, we obtain a weak same-sign preference for transfer terms:

$$\log \text{BF}_{\text{transfer/no-transfer}} \approx +0.24. \quad (12)$$

In the all-transfer variant (SN+BAO+CC+ladder term), the score is mildly negative:

$$\log \text{BF}_{\text{transfer/no-transfer}} \approx -0.48. \quad (13)$$

This is compatible with a small inference-bias contribution in SN-only compression, but not a decisive multi-probe detection at current calibration depth.

**High-leverage-event jackknife stability.** For the O3 selection-function-calibrated configuration, the full score is

$$\Delta \text{LPD}_{\text{full}} = 3.67. \quad (14)$$

Dropping the highest-leverage event (GW200308\_173609) gives

$$\Delta \text{LPD}_{\text{drop 1}} = 2.19, \quad (15)$$

and an approximate top-2 leave-out gives

$$\Delta \text{LPD}_{\text{drop 2}} \approx 1.70. \quad (16)$$

The signal is therefore concentrated in a small subset of high-leverage events, but it does not collapse when the top event is removed.

**Nonlinear bridge scan.** Using a late-transition profile

$$\alpha(z) = \alpha_{\text{high}} + \frac{\alpha_{\text{low}} - \alpha_{\text{high}}}{1 + \exp[(z - z_t)/w]}, \quad (17)$$

we find broad viable families that satisfy growth/lensing consistency near  $\alpha_{\text{eff}} \sim 0.6$  while reaching material-relief targets near  $\alpha_{\text{relief,eff}} \sim 1.94$  to 1.95 in low- $z$  windows. A representative solution is

$$(\alpha_{\text{high}}, \alpha_{\text{low}}, z_t, w) \approx (0.60, 1.95, 0.26, 0.03), \quad (18)$$

with comparable neighboring solutions for other low- $z$  effective windows.

**Entropy-anchored direct dark-siren re-score.** We also replaced the phenomenological propagation posterior with the entropy-reconstruction posterior from the submission-hardening run and re-scored the same O3 selection-function-calibrated dark-siren set. The total support remains positive but is reduced:

$$\Delta \text{LPD}_{\text{entropy direct}} = 2.26 \quad (\text{vs. } 3.67 \text{ baseline}). \quad (19)$$

The same highest-leverage event remains GW200308\_173609; leave-one-out gives

$$\Delta \text{LPD}_{\text{entropy, drop GW200308}} = 1.20. \quad (20)$$

Numerically this is about 0.62 of the baseline support, consistent with the entropy-alignment quick test indicating effective amplitudes below the material-relief scale.

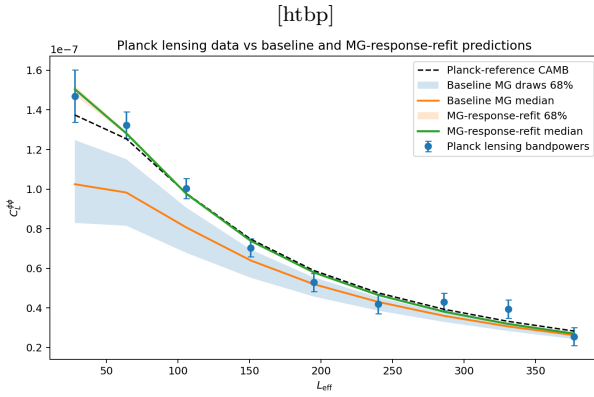


**Figure 3.** Planck 2018 lensing bandpowers with baseline MG projection and MG-aware refit overlay. The refit absorbs the baseline suppression and restores near-reference fit quality.

## 4 DISCUSSION AND CONCLUSIONS

The central result is that GR-assumed standard-ruler inversion can introduce a tension-scale inference bias in  $H_0$  if GW propagation is modified at the level implied by the adopted template. In this framework, the induced shift is of order  $+2$  to  $+5 \text{ km s}^{-1} \text{ Mpc}^{-1}$ .

Direct friction closure is smaller, with  $\mathcal{R}_{\text{anchor}}^{\text{GR}} \simeq 0.16$ . The dominant mechanism in this Letter is therefore not late-time closure by friction alone, but the parameter wedge created by a mismatched inference model: GR compression can separate early and late anchors even when the underlying cosmology is internally consistent under MG truth.

This interpretation is compatible with our lensing and stability checks. Baseline lensing projection is suppressed, but MG-aware response freedom restores near-reference performance. Pantheon SN-only transfer is weakly same-sign while the all-transfer variant is mildly negative, so present electromagnetic-sector evidence remains suggestive rather than decisive. Jackknife tests show concentration in GW200308\_173609 and other high-leverage events, but no single-event collapse.

The identified vulnerabilities correspond to explicit, near-term tests. If the propagation deviation is physical, the population-level preference should stabilise (and should become less dominated by single events) as the siren sample grows and galaxy-catalogue completeness and selection modelling improve in O4/O5. Similarly, the degree of lensing response freedom required to reconcile baseline suppression with Planck 2018 lensing can be confronted with higher-precision CMB lensing measurements and joint large-scale-structure combinations, which should either recover a consistent MG response or exclude the relevant parameter space.

Even if the GWTC-3 propagation preference is ultimately attributed to residual systematics, the mapping derived here quantifies the magnitude of bias that would follow from a propagation deviation of comparable form, and motivates treating GR propagation as an explicit assumption to be stress-tested in standard-siren cosmology. If the signal persists in larger siren samples, corrected dark-siren inference no longer requires a universally high late-time  $H_0$ , and the remaining discrepancy is more naturally isolated to the elec-

tromagnetic calibration/propagation sector rather than to a single global expansion-history failure.

## ACKNOWLEDGEMENTS

The author used AI-assisted tools for drafting, editing, and software development.

## DATA AVAILABILITY AND DOIS

All code and reproducibility artefacts used in this study are archived at Zenodo, DOI [10.5281/zenodo.18603134](https://doi.org/10.5281/zenodo.18603134). Upstream O3 search-sensitivity injections are available at DOI [10.5281/zenodo.7890437](https://doi.org/10.5281/zenodo.7890437). Public cosmological datasets used here are cited in the reference list with corresponding DOIs.

## REFERENCES

- R. Abbott *et al.* (LIGO Scientific Collaboration, Virgo Collaboration, and KAGRA Collaboration), “GWTC-3: Compact Binary Coalescences Observed by LIGO and Virgo During the Second Part of the Third Observing Run,” *Phys. Rev. X* **13**, 041039 (2023), DOI: [10.1103/PhysRevX.13.041039](https://doi.org/10.1103/PhysRevX.13.041039).
- N. Aghanim *et al.* (Planck Collaboration), “Planck 2018 results. VI. Cosmological parameters,” *Astron. Astrophys.* **641**, A6 (2020), DOI: [10.1051/0004-6361/201833910](https://doi.org/10.1051/0004-6361/201833910).
- N. Aghanim *et al.* (Planck Collaboration), “Planck 2018 results. VIII. Gravitational lensing,” *Astron. Astrophys.* **641**, A8 (2020), DOI: [10.1051/0004-6361/201833886](https://doi.org/10.1051/0004-6361/201833886).
- S. Alam *et al.*, “The clustering of galaxies in the completed SDSS-III Baryon Oscillation Spectroscopic Survey: cosmological analysis of the DR12 galaxy sample,” *Mon. Not. R. Astron. Soc.* **470**, 2617 (2017), DOI: [10.1093/mnras/stx721](https://doi.org/10.1093/mnras/stx721).
- S. Alam *et al.*, “Completed SDSS-IV extended Baryon Oscillation Spectroscopic Survey: Cosmological implications from two decades of spectroscopic surveys at the Apache Point Observatory,” *Phys. Rev. D* **103**, 083533 (2021), DOI: [10.1103/PhysRevD.103.083533](https://doi.org/10.1103/PhysRevD.103.083533).
- E. Belgacem, Y. Dirian, S. Foffa, and M. Maggiore, “Modified gravitational-wave propagation and standard sirens,” *Phys. Rev. D* **98**, 023510 (2018), DOI: [10.1103/PhysRevD.98.023510](https://doi.org/10.1103/PhysRevD.98.023510).
- E. Bellini and I. Sawicki, “Maximal freedom at minimum cost: linear large-scale structure in general modifications of gravity,” *J. Cosmol. Astropart. Phys.* **07** (2014) 050, DOI: [10.1088/1475-7516/2014/07/050](https://doi.org/10.1088/1475-7516/2014/07/050).
- D. Brout *et al.*, “The Pantheon+ Analysis: Cosmological Constraints,” *Astrophys. J.* **938**, 110 (2022), DOI: [10.3847/1538-4357/ac8e04](https://doi.org/10.3847/1538-4357/ac8e04).
- DESI Collaboration, “DESI 2024 VI: cosmological constraints from the measurements of baryon acoustic oscillations,” *J. Cosmol. Astropart. Phys.* **02** (2025) 021, DOI: [10.1088/1475-7516/2025/02/021](https://doi.org/10.1088/1475-7516/2025/02/021).
- W. L. Freedman *et al.*, “The Carnegie-Chicago Hubble Program. VIII. An independent determination of the Hubble constant based on the tip of the red giant branch,” *Astrophys. J.* **882**, 34 (2019), DOI: [10.3847/1538-4357/ab2f73](https://doi.org/10.3847/1538-4357/ab2f73).
- LIGO Scientific Collaboration, Virgo Collaboration, and KAGRA Collaboration, “GWTC-3: Compact Binary Coalescences Observed by LIGO and Virgo During the Second Part of the Third Observing Run — O3 search sensitivity estimates,” Zenodo (2023), DOI: [10.5281/zenodo.7890437](https://doi.org/10.5281/zenodo.7890437).
- M. Moresco *et al.*, “Improved constraints on the expansion rate of the Universe up to  $z \sim 1.1$  from the spectroscopic evolution of

- cosmic chronometers,” *J. Cosmol. Astropart. Phys.* **08** (2012) 006, DOI: [10.1088/1475-7516/2012/08/006](https://doi.org/10.1088/1475-7516/2012/08/006).
- A. Nishizawa, “Generalized framework for testing gravity with gravitational-wave propagation,” *Phys. Rev. D* **97**, 104037 (2018), DOI: [10.1103/PhysRevD.97.104037](https://doi.org/10.1103/PhysRevD.97.104037).
- L. Pogosian and A. Silvestri, “What can cosmology tell us about gravity? Constraining Horndeski gravity with  $\Sigma$  and  $\mu$ ,” *Phys. Rev. D* **94**, 104014 (2016), DOI: [10.1103/PhysRevD.94.104014](https://doi.org/10.1103/PhysRevD.94.104014).
- A. G. Riess *et al.*, “A Comprehensive Measurement of the Local Value of the Hubble Constant with  $1 \text{ km s}^{-1} \text{ Mpc}^{-1}$  Uncertainty from the Hubble Space Telescope and the SH0ES Team,” *Astrophys. J. Lett.* **934**, L7 (2022), DOI: [10.3847/2041-8213/ac5c5b](https://doi.org/10.3847/2041-8213/ac5c5b).
- J. Simon, L. Verde, and R. Jimenez, “Constraints on the redshift dependence of the dark energy potential,” *Phys. Rev. D* **71**, 123001 (2005), DOI: [10.1103/PhysRevD.71.123001](https://doi.org/10.1103/PhysRevD.71.123001).
- A. B. Smith, “O3 Modified Gravity Tension Replication,” Zenodo (2026), DOI: [10.5281/zenodo.18603134](https://doi.org/10.5281/zenodo.18603134).
- D. Stern *et al.*, “Cosmic chronometers: constraining the equation of state of dark energy. I:  $H(z)$  measurements,” *J. Cosmol. Astropart. Phys.* **02** (2010) 008, DOI: [10.1088/1475-7516/2010/02/008](https://doi.org/10.1088/1475-7516/2010/02/008).